Molecular Pharmacology Fast Forward. Published on January 19, 2010 as doi:10.1124/mol.109.061010

MOL #61010

15-Deoxy-$\Delta^{12,14}$-Prostaglandin J_2 Biphasically Regulates the Proliferation of Mouse Hippocampal Neural Progenitor Cells by Modulating the Redox State

Takashi Katura, Takahiro Moriya, Norimichi Nakahata

Department of Cellular Signaling, Graduate School of Pharmaceutical Sciences, Tohoku University, Sendai, Japan

Molecular Pharmacology Fast Forward. Published on January 19, 2010 as DOI: 10.1124/mol.109.061010
This article has not been copyedited and formatted. The final version may differ from this version.

Running title: Regulation of neural progenitor proliferation by 15d-PGJ_2

Address correspondence to: Takahiro Moriya, Ph. D., Department of Cellular Signaling, Graduate School of Pharmaceutical Sciences, Tohoku University, Aoba 6-3, Aramaki, Aoba-ku, Sendai 980-8578, Japan. Tel. +81-22-795-3843; Fax. +81-22-795-3847; E-mail: moriya@mail.pharm.tohoku.ac.jp

Number of text pages: 48

Number of tables: 0

Number of figures: 8

Number of supplemental figures: 5

Number of references: 40

Number of words in Abstract: 228

Number of words in Introduction: 500

Number of words in Discussion: 1203

Abbreviations used: 15d-PGJ_2, 15-deoxy-$\Delta^{12,14}$-prostaglandin J_2; BrdU, bromodeoxyuridine; BSA, bovine serum albumin; CAY10410, 9,10-dehydro-15-deoxy-$\Delta^{12,14}$-prostaglandin J_2; COX-2, cyclooxygenase-2; DG, dentate gyrus; DP1, prostaglandin D_2 receptor type 1; DP2, prostaglandin D_2 receptor type 2; DTNB, 5,5'-dithiobis[2-nitrobenzoic acid]; EGF, epidermal growth factor; FGF2, fibroblast growth factor 2; GFAP, glial fibrillary acidic protein; GSH, glutathione; GSH-EE, glutathione ethyl ester; H_2DCFDA, 2',7'-dichlorodihydrofluorescein diacetate; LPS, lipopolysaccharide; MHM, media-hormone-mix; NPCs, neural progenitor cells; PB, phosphate buffer; PBS,

Molecular Pharmacology Fast Forward. Published on January 19, 2010 as DOI: 10.1124/mol.109.061010
This article has not been copyedited and formatted. The final version may differ from this version.

phosphate-buffered saline; PBSBT, PBS containing 0.5% BSA and 0.3% Triton X-100; PBSGT, PBS containing 1% normal goat serum and 0.3% Triton X-100; PFA, paraformaldehyde; PGD_2, prostaglandin D_2; PGs, prostaglandins; PMA, phorbol 12,13-myristate acetate; PPARγ, peroxisome proliferator-activated receptor γ; ROS, reactive oxygen species; SGZ, subgranular zone; SVZ, subventricular zone; Trx, thioredoxin; Tuj1, β-tubulin type III.

Molecular Pharmacology Fast Forward. Published on January 19, 2010 as DOI: 10.1124/mol.109.061010
This article has not been copyedited and formatted. The final version may differ from this version.

Abstract

The activity of neural progenitor cells (NPCs) is regulated by various humoral factors. Although prostaglandin D_2 (PGD_2) is known to mediate various physiological brain functions such as sleep, its actions on NPCs have not been fully understood. In the process of investigating the effects of PGD_2 on NPCs, we found that 15-deoxy-$\Delta^{12,14}$-prostaglandin J_2 (15d-PGJ_2), an endogenous metabolite of PGD_2, exhibits a novel regulation of the proliferation of NPCs derived from mouse hippocampus. 15d-PGJ_2 showed biphasic effects on EGF-induced proliferation of NPCs; facilitation at low concentrations (around 0.3 μM) and suppression at higher concentrations (0.5 – 10 μM) *in vitro*. GW9662, an inhibitor of peroxisome proliferator-activated receptor γ (PPARγ), known to be a molecular target for 15d-PGJ_2, failed to abolish the effects of 15d-PGJ_2. CAY10410, a structural analog of 15d-PGJ_2 lacking the electrophilic carbon in the cyclopentenone ring, did not show 15d-PGJ_2-like actions. Treatment with 15d-PGJ_2 increased the levels of reactive oxygen species (ROS) and decreased endogenous glutathione (GSH) levels. Furthermore, supplementation with a membrane-permeable analog of glutathione, GSH ethyl ester (GSH-EE) (2 mM), diminished the biphasic effects of 15d-PGJ_2. Finally, cell division in the dentate gyrus of postnatal mice was increased by i.c.v. injection of low-dose (1 ng) 15d-PGJ_2 and suppressed by high-dose (30 ng) 15d-PGJ_2. These results suggest that 15d-PGJ_2 regulates the proliferation of NPCs via its electrophilic nature, which enables covalent binding to molecules such as GSH.

Molecular Pharmacology Fast Forward. Published on January 19, 2010 as DOI: 10.1124/mol.109.061010
This article has not been copyedited and formatted. The final version may differ from this version.

Introduction

Recent extensive studies have elucidated that three cell types in the brain (neurons, astrocytes and oligodendrocytes) originate from immature precursor cells referred to as neural progenitor cells (NPCs) (Gage, 2000; Weiss et al., 1996). During development, NPCs primarily undergo extensive self-renewal and then generate neurons; later, they sequentially generate astrocytes and oligodendrocytes (Miller and Gauthier, 2007). NPCs are located not only in the developing mammalian brain but also in the adult brain, and are especially abundant in the anterior subventricular zone (SVZ) and subgranular zone (SGZ) of the hippocampal dentate gyrus (DG) (Eriksson et al., 1998). The self-renewal and multipotential activities of NPCs are dynamically regulated by various humoral factors under physiological and pathophysiological conditions, such as ischemia (Nakatomi et al., 2002), seizure (Parent et al., 1997) and sleep (Guzman-Marin et al., 2003). The elucidation of signaling molecules regulating NPC activity may contribute not only to the understanding of neurogenesis but also toward the development of new therapies against nervous system disorders; however, the cellular mechanisms underlying regulation of NPC activity have not been fully understood.

Prostaglandins (PGs) are a group of 20-carbon fatty acids that are produced within cells via the cyclooxygenase pathway from arachidonic acid in response to a variety of

Molecular Pharmacology Fast Forward. Published on January 19, 2010 as DOI: 10.1124/mol.109.061010
This article has not been copyedited and formatted. The final version may differ from this version.

extrinsic stimuli (Smith, 1989; Smith, 1992), and some PGs such as PGE_2 are reported to regulate the activity of NPCs (Uchida et al., 2002). Prostaglandin D_2 (PGD_2) is considered to be a molecular candidate regulating NPCs, because it is the most abundant PG in the brain (Ogorochi et al., 1984) and is known to play critical roles in sleep (Hayaishi, 2002; Herlong and Scott, 2006; Huang et al., 2007), which drastically alters NPC activity (Guzman-Marin et al., 2003). In the process of investigating the effects of sleep-related factors on the proliferation of mouse hippocampal NPCs, we observed that PGD_2 showed biphasic actions on NPC proliferation (Supplemental Fig. 1). Furthermore, we found that 15-deoxy-$\Delta^{12,14}$-prostaglandin J_2 (15d-PGJ_2), a non-enzymatic metabolite of PGD_2, exhibited a novel regulation of the proliferation of NPCs. 15d-PGJ_2 is endogenously produced from PGD_2 through spontaneous nonenzymatic dehydration followed by isomerization and is an endogenous ligand for peroxisome proliferator-activated receptor γ (PPARγ) (Forman et al., 1995), which plays a critical role in the regulation of cell differentiation and metabolism (Debril et al., 2001; Walczak and Tontonoz, 2002). On the other hand, it is also reported that 15d-PGJ_2 covalently binds with nucleophilic molecules such as glutathione (GSH) via an electrophilic carbon at position 9 in its cyclopentenone ring (Oliva et al., 2003; Rossi et al., 2000; Straus et al., 2000). GSH is known to be a major endogenous antioxidant that

Molecular Pharmacology Fast Forward. Published on January 19, 2010 as DOI: 10.1124/mol.109.061010
This article has not been copyedited and formatted. The final version may differ from this version.

protects cells from reactive oxygen species (ROS) such as free radicals and peroxides (Shibata et al., 2003); thus, decreases in GSH levels would lead to the elevation of ROS levels. At present, little is known about the effects of 15d-PGJ_2 on the activity of NPCs. In this study, we examined the mode of 15d-PGJ_2 actions on the proliferation of mouse hippocampal NPCs *in vitro* and *in vivo*.

Materials and Methods

Animals. Timed-pregnant female and young male (5 weeks) ICR mice (SLC, Shizuoka, Japan) were used. All mice were housed in polypropylene cages (31 × 22 × 14 cm) with wood shavings, and were maintained in an environment with a controlled temperature (23±2°C) and light (12:12 h light:dark). Food and water were available *ad libitum*. All animal housing and surgical procedures were performed in accordance with the guidelines of the Japanese Pharmacological Society and were approved by the Institutional Animal Care and Use Committee of the Graduate School of Pharmaceutical Sciences, Tohoku University.

Cell culture. NPCs were isolated and propagated by a neurosphere method as reported previously (Reynolds et al., 1992) with minor modifications (Moriya et al., 2007). Fetuses on embryonic day 15.5 (embryonic day 0 is defined as midnight on the day of overnight mating) were isolated from their mothers under deep anesthesia with diethyl ether and placed into an ice-cold 1:1 mixture of Dulbecco's modified Eagle's medium and F-12 nutrient (DMEM/F-12; Gibco-BRL, Gaithersburg, Md., USA). The hippocampal tissues were carefully micro-dissected using a stereomicroscope and triturated with a 1-ml plastic pipette to obtain a single cell suspension in media-hormone-mix (MHM) (DMEM/F-12 supplemented with 0.34% glucose, 23

Molecular Pharmacology Fast Forward. Published on January 19, 2010 as DOI: 10.1124/mol.109.061010
This article has not been copyedited and formatted. The final version may differ from this version.

μg/ml insulin, 92 μg/ml transferrin, 55 μM putrescine, 27.5 nM sodium selenite, 20 nM progesterone, 50 U/ml penicillin, 50 μg/ml streptomycin). The viable dissociated cells at a density of 4 x 10^5 cells/ml (total 12 ml) in MHM containing 20 ng/ml epidermal growth factor (EGF) (Invitrogen Corp., Carlsbad, CA, USA) and 20 ng/ml fibroblast growth factor 2 (FGF2) (Peprotech EC, London, UK) were seeded into uncoated T75 culture flasks (Becton-Dickinson, Franklin Lake, NJ, USA) and were maintained in a humidified incubator at 37°C with 95% atmospheric air and 5% CO_2. The cells were fed 3 ml of fresh medium every second day and were incubated for 5 days to form a sufficient number of neurospheres.

Reagents. 15d-PGJ_2, BWA868C, and CAY10410 were purchased from Cayman Chemical (Ann Arbor, MI, USA) and were dissolved in ethanol. Ramatroban was kindly provided by Bayer Yakuhin (Osaka, Japan) and was dissolved in ethanol. GW9662 was purchased from ALEXIS Biochemicals (San Diego, CA, USA) and was dissolved in ethanol. Bromodeoxyuridine (BrdU) was purchased from Nacalai Tesque (Kyoto, Japan). Alexa488-conjugated goat anti-mouse IgG, Alexa568-conjugated goat anti-rabbit IgG, Alexa568-conjugated goat anti-rat IgG and 2',7'-dichlorodihydrofluorescein diacetate (H_2DCFDA) were purchased from Molecular Probes (Eugene, OR, USA). Mouse anti-β-tubulin type III (Tuj1), rabbit anti-glial

Molecular Pharmacology Fast Forward. Published on January 19, 2010 as DOI: 10.1124/mol.109.061010
This article has not been copyedited and formatted. The final version may differ from this version.

fibrillary acidic protein (GFAP), GSH reduced ethyl ester (GSH-EE), β-NADPH, 5,5'-dithiobis[2-nitrobenzoic acid] (DTNB), sulfosalicylic acid (Dayer et al.) and GSH reductase were purchased from Sigma-Aldrich (St. Louis, MO, USA). Mouse anti-nestin monoclonal antibody was purchased from Chemicon (Massachusetts, USA).

Experimental procedure. The effects of 15d-PGJ_2 on the proliferation of NPCs were evaluated by two methods: a) indirect measurement of the number of viable cells by WST-8 assay; and b) a BrdU incorporation assay. We did not adopt direct and simple counting of cell number because 1) NPCs form colonies (spheres), that prevent us from measuring cell number without enzymatic dissociation, and 2) dead cells especially appeared under EGF-free conditions or in the presence of a high concentration of 15d-PGJ_2, and these could not be discriminated from viable cells. As described later, although the WST-8 assay is widely used for measuring relative numbers of NPCs (Jiang et al., 2005; Kanemura et al., 2002; Moriya et al., 2007), it measures the metabolic activity of cells. Therefore, we also examined DNA synthesis activity using a BrdU incorporation assay to confirm the results of the WST-8 assay. Single cell suspensions from primary neurospheres were prepared by centrifugation (300 × g, 5 min) followed by enzymatic dissociation with collagenase (1 mg/ml). The cells were then allowed to pass through a 40-μm nylon net and were seeded in non-treatment

Molecular Pharmacology Fast Forward. Published on January 19, 2010 as DOI: 10.1124/mol.109.061010
This article has not been copyedited and formatted. The final version may differ from this version.

96-well plates (Becton-Dickson) at a density of 1 x 10^5 cells/ml, and incubated for 12 h in the absence of EGF. Thereafter, they were stimulated with or without various concentrations of 15d-PGJ_2 (0.01–10 μM), PGD_2 (0.1–10 μM) or CAY10410 (0.01–10 μM) in the presence (2 or 20 ng/ml) or absence of EGF. In some experiments, cells were pretreated with the DP1 antagonist BWA868C (10 μM), the DP2 antagonist ramatroban (10 μM) or the PPARγ antagonist GW9662 (0.1 μM) for 1 h prior to 15d-PGJ_2 or PGD_2 stimulation.

WST-8 assay. The number of viable cells was indirectly estimated by the WST-8 assay using a Cell Counting Kit-SF (Nacalai Tesque), which has been used for to estimate the proliferative activity of NPSs cultured by the neurosphere method (Jiang et al., 2005; Kanemura et al., 2002; Moriya et al., 2007). WST-8 is reduced by the mitochondrial enzyme, NAD-dependent succinate dehydrogenase, to form a colored formazan product, which is soluble in the culture medium. The amount of formazan dye generated by the activity of the dehydrogenases in cells is known to be directly proportional to the number of living cells (Jiang et al., 2005). It has been reported that indirect measurements of viable cells based on metabolic activity are effective and reproducible ways to determine the numbers of viable cells, especially of viable NPCs present within intact neurospheres, without breaking the neurospheres (Kanemura et al.,

Molecular Pharmacology Fast Forward. Published on January 19, 2010 as DOI: 10.1124/mol.109.061010
This article has not been copyedited and formatted. The final version may differ from this version.

2002). After NPCs were treated as described above for 48 h, 5 µl of the Cell Counting Kit solution was added to each well and incubated for an additional 5 h at 37°C. The absorbance at 450 nm with a reference wavelength of 595 nm was measured using a microplate reader (TECAN, Austria) and the net absorbance subtracting the values of cell-free wells was calculated.

BrdU incorporation assay. After incubation in the absence of EGF for 12 h, NPCs were treated with or without various concentrations of 15d-PGJ_2 in the presence or absence of EGF for 48 h. BrdU (1 µM) was added to the culture medium for the appropriate length of time. Subsequently, cells were fixed with 4% paraformaldehyde (PFA) for 15 min, washed with phosphate-buffered saline (PBS), and then permeabilized by incubation with 2 N HCl at 37°C for 5 min. After removal of HCl, they were washed with 0.15 M sodium borate (pH 8.5) at room temperature for 10 min. They were then incubated with PBS containing 1% normal goat serum and 0.3% Triton X-100 (PBSGT) for 2 h, and incubated overnight with rat anti-BrdU antibody (1:200; Oxford Biotechnology, Kidlington U.K.) in PBSGT at 4°C. After removal of the primary antibody solution, cells were washed with PBS and incubated with secondary antibody (Alexa568-conjugated goat anti-rat IgG, 1:200) and 1 µg/ml Hoechst 33258 for nuclear counterstaining, for 2 h at room temperature under light-shading conditions.

Molecular Pharmacology Fast Forward. Published on January 19, 2010 as DOI: 10.1124/mol.109.061010
This article has not been copyedited and formatted. The final version may differ from this version.

After washing cells with PBS, fluorescent images were automatically obtained using the CelaView imaging system (Olympus, Tokyo, Japan) and the numbers of BrdU-labeled cells and Hoechst-stained nuclei were automatically counted by the Scan® system (Olympus).

TUNEL staining. TUNEL staining was performed using the In Situ Cell Death Detection Kit, TMR red (Roche, Mannheim, Germany) according to the manufacturer's instructions. Briefly, the dispersed NPCs from the primary neurospheres were seeded into Lab-Tek® chamber Slides™ (Nunc, Inc., Naperville, IL, USA) pre-coated with 30 μg/ml poly-L-lysine (Sigma) and 15 μg/ml laminin at a density of 4×10^5 cells/ml for 12 h incubation period in the absence of EGF. After NPCs were treated with or without of various concentrations of 15d-PGJ_2 in the presence of EGF (2 ng/ml) for 48 h, they were fixed with 4% PFA for 15 min and then washed with PBS. After permeabilization with 0.1% citrate buffer containing 0.1% Triton X-100 for 2 min on ice, the cells were incubated with TUNEL mix for 1 h at 37°C, and then washed with PBS. Thereafter, Hoechst 33258 was added to cells at a concentration of 1 μg/ml. After washing with PBS, the cover slips were mounted on glass slides. The images in nine randomly-selected areas (each; 350 x 350 μm) for each well were obtained using a fluorescence microscope (10 × objective lens, IX70, Olympus) and the numbers of

Molecular Pharmacology Fast Forward. Published on January 19, 2010 as DOI: 10.1124/mol.109.061010
This article has not been copyedited and formatted. The final version may differ from this version.

TUNEL-positive cells and total cells stained with Hoechst dye were counted by an observer without knowledge of the treatment.

Reactive oxygen species (ROS) measurement. ROS levels in NPCs were measured using the fluorescence probe H_2DCFDA. After incubation in the absence of EGF for 12 h, NPCs were treated with or without various concentrations of 15d-PGJ_2, CAY10410, phorbol 12,13-myristate acetate (PMA) and/or GSH-EE in the presence of EGF (2 ng/ml) for 2 h. H_2DCFDA (10 μM) was added to cells during the last 30 min of the incubation period. Immediately after washing cells with MHM, fluorescent images were obtained using a fluorescence microscope (IX70, Olympus) and the numbers of H_2DCFDA-positive cells and the level of fluorescence intensity per cell were evaluated by Scion® Image (Olympus).

Total intracellular GSH measurement. NPCs were treated with or without various concentrations of 15d-PGJ_2 in the presence of EGF (2 ng/ml) for 12 h. The cells were lysed in 5% 5-sulfosalicylic acid solution. The samples were incubated with working solution (6 units/ml GSH reductase and 1.5 mg/ml DTNB in 0.1 M potassium phosphate buffer with 1 mM EDTA) for 5 min followed by addition of 0.16 mg/ml β-NADPH. The total GSH levels were determined by measuring the absorbance at 412 nm with a TECAN microplate reader and the concentration of total GSH (nmoles/ml) was

Molecular Pharmacology Fast Forward. Published on January 19, 2010 as DOI: 10.1124/mol.109.061010
This article has not been copyedited and formatted. The final version may differ from this version.

calculated based on a reduced glutathione standard curve. The protein concentrations of the cell lysates were determined by DC protein assay and the total contents of GSH, including both reduced glutathione and oxidized glutathione (nmoles/mg protein), were calculated.

Differentiation assay. NPCs were seeded into 96-well plates (Nunc) pre-coated with 30 μg/ml poly-L-lysine followed by 15 μg/ml laminin, and incubated for 12 h in the presence of EGF (2 ng/ml). Then, NPCs were treated with or without various concentrations of 15d-PGJ_2 in the absence of EGF for 96 h. Thereafter, NPCs were fixed with 4% PFA for 15 min and then washed with PBS. They were incubated with PBS containing 0.5% bovine serum albumin (BSA) and 0.3% Triton X-100 (PBSBT) for 2 h, and incubated overnight with primary antibody (mouse anti-Tuj1, 1:200, and rabbit anti-GFAP, 1:200) in PBSBT at 4°C. After removal of the primary antibody solution, cells were washed with PBS and incubated with secondary antibody (Alexa488-conjugated goat anti-mouse IgG, 1:200, and Alexa568-conjugated goat anti-rabbit IgG, 1:200) and 1 μg/ml Hoechst 33258 for nuclear counterstaining, for 2 h at room temperature under light-shading conditions. After washing cells with PBS, fluorescent images were automatically obtained using the CelaView imaging system (Olympus) and the numbers of Tuj1- and GFAP-positive cells as well as the numbers of

Molecular Pharmacology Fast Forward. Published on January 19, 2010 as DOI: 10.1124/mol.109.061010
This article has not been copyedited and formatted. The final version may differ from this version.

Hoechst-stained nuclei were counted by the Scan® system (Olympus).

Nestin staining. NPCs were seeded in Lab-Tek® chamber Slides™ pre-coated with 30 μg/ml poly-L-lysine followed by 15 μg/ml laminin. Then, NPCs were treated with medium in the absence of EGF for 2 h. Thereafter, NPCs were fixed with 4% PFA for 15 min and washed with PBS. The cells were stained using primary antibody (mouse anti-nestin; 1:300) and secondary antibody (Alexa488-conjugated goat anti-mouse IgG; 1:200) and 1 μg/ml Hoechst 33258 as described above.

Schedule of drug treatment and sampling *in vivo*. Male ICR mice at 5 weeks of age were intracerebroventricularly administered vehicle or 15d-PGJ_2 (0–30 ng/3 μl saline per mouse) and were intraperitoneally injected with BrdU (50 mg/kg), 5 h or 24 h after 15d-PGJ_2 injection. Two hours after BrdU injection, mice were deeply anesthetized with diethyl ether and then perfused intracardially with 25 ml of chilled saline followed by 25 ml of 4% PFA in 0.1 M phosphate buffer (PB). Thereafter, their brains were quickly removed.

Immunohistochemistry. The brains were post-fixed with 4% PFA in 0.1 M PB overnight at 4°C, followed by immersion in 20% sucrose in 0.1 M PB for 48 h. The brains were cut into 40-μm sections from the rostral to the caudal edge of the dentate gyrus using a cryostat (MICROM HM560, Mikron Instrument, Inc., CA) and the

Molecular Pharmacology Fast Forward. Published on January 19, 2010 as DOI: 10.1124/mol.109.061010
This article has not been copyedited and formatted. The final version may differ from this version.

sections were alternately divided into two groups. For BrdU immunohistochemistry, one group of sections was treated with HCl (2 N) at 37°C for 20 min, then neutralized twice with sodium borate buffer (0.15 M, pH 8.5) at room temperature for 10 min. After three washes with PBS, the sections were incubated with rat anti-BrdU antibody (1:200) diluted with PBSGT at 4°C overnight, followed by Alexa568-conjugated goat anti-rat IgG (1:200) and 1 μg/ml Hoechst 33258, diluted with PBSGT at room temperature for 2 h.

Quantification of the number of BrdU-labeled cells. The numbers of BrdU-labeled cells were counted using a 10 × objective (IX70, Olympus, Tokyo, Japan) throughout the rostrocaudal extent of the dentate gyrus. We counted the number of BrdU-labeled cells in the SGZ, which was defined as a 2-cell body wide zone (approximately 10 μm) along the border of the GCL and the hilus. Because we stained every second section, resulting numbers were then multiplied by two to obtain the estimated total number of BrdU-labeled cells per dentate gyrus. The counting was performed by an observer without any knowledge of the experimental groups.

Statistical analysis. Results are expressed as the means ± SEM. The statistical significance of differences was determined by one-way ANOVA followed by Dunnett's test or Fisher's PLSD test. Results were considered to be significant if the *p* value was

Molecular Pharmacology Fast Forward. Published on January 19, 2010 as DOI: 10.1124/mol.109.061010
This article has not been copyedited and formatted. The final version may differ from this version.

less than 0.05.

Molecular Pharmacology Fast Forward. Published on January 19, 2010 as DOI: 10.1124/mol.109.061010
This article has not been copyedited and formatted. The final version may differ from this version.

Results

The effect of 15d-PGJ_2 on EGF-induced proliferation of cultured hippocampal NPCs. We expanded NPCs from embryonic mouse hippocampus using the neurosphere method and confirmed that a large proportion of neurosphere cells (95.3 ± 0.73%) expressed nestin, a marker for NPCs under our experimental conditions. In our pilot study investigating the effects of sleep-related compounds on the proliferation of cultured NPCs from embryonic mouse hippocampus, we observed that PGD_2 exhibited biphasic actions on the proliferation of NPCs. In examining the effects of PGD_2 and 15d-PGJ_2, we used not only the most popular concentration of EGF (20 ng/ml), but also a relatively low concentration of EGF (2 ng/ml) as well as EGF-free conditions, because it has been reported that the growth-promoting activity of EGF on embryonic brain-derived neurospheres shows a concentration dependency between 0.5 ng/ml and 20 ng/ml (Tropepe et al., 1999), and a submaximal concentration of 2 ng/ml was considered to be optimal for finding the accelerative and/or suppressive potential of PG on the proliferation of NPCs. As shown in Supplemental Fig. 1, PGD_2 increased the number of NPCs when present at a concentration of around 2 μM, but decreased it when present at concentrations of over 3 μM in the presence of EGF (2 and 20 ng/ml). The maximum increase by PGD_2 was greater in the 2 ng/ml EGF condition (190%) than in

Molecular Pharmacology Fast Forward. Published on January 19, 2010 as DOI: 10.1124/mol.109.061010
This article has not been copyedited and formatted. The final version may differ from this version.

the 20 ng/ml condition (133%) (Supplemental Fig. 1). Under the EGF-free condition, PGD_2 increased cell number at concentrations of 2–3 μM, but did not decrease it at high concentrations (Supplemental Fig. 1). Because PGD_2 has been reported to be a ligand for two types of G-protein-coupled receptors (DP1 and DP2), we investigated the effects of a DP1 antagonist (BWA868C) and a DP2 antagonist (ramatroban) on the regulation of proliferation by PGD_2 (Supplemental Fig. 1). Although there were some significant differences between the vehicle and antagonist groups at each concentration of PGD_2 (BWA868C; 1 μM in 2 ng/ml EGF, 3 μM and 5 μM in 20 ng/ml EGF, ramatroban; 0.1 μM in 0 ng/ml EGF, 0.1, 0.3 and 2 μM in 2 ng/ml EGF and 5 μM in 20 ng/ml EGF, $p < 0.05$, Student's *t*-test, significant marks not shown in figure), the biphasic actions of PGD_2 on proliferation of NPCs were still evident in each BWA868C and ramatroban group (Supplemental Fig. 1). These results suggest that neither DP1 nor DP2 mediates the effects of PGD_2 on the proliferation of NPCs.

We next examined the effect of 15d-PGJ_2 on the self-renewal ability of cultured hippocampal NPCs, because PGD_2 is reported to be non-enzymatically converted to 15d-PGJ_2 even in culture medium (Shibata et al., 2002). We employed the WST-8 assay, which indirectly measures the viable cell number based on their metabolic activity. EGF increased the number of viable cells in a concentration-dependent manner (Fig. 1A). In

Molecular Pharmacology Fast Forward. Published on January 19, 2010 as DOI: 10.1124/mol.109.061010
This article has not been copyedited and formatted. The final version may differ from this version.

the presence of EGF (2 and 20 ng/ml), 15d-PGJ_2 at low concentrations (around 0.3 μM) significantly increased the number of viable cells, whereas at high concentrations (0.5–10 μM), it significantly reduced the number of viable cells. In contrast to PGD_2, 15d-PGJ_2 at lower concentrations failed to increase the cell number under EGF-free conditions; however, it reduced the number of viable cells at high concentrations (1–10 μM). These results show that 15d-PGJ_2 exhibits biphasic actions on EGF-induced increase in viable NPC number. The increase in NPC number induced by 15d-PGJ_2 was more marked in the presence of a low concentration of EGF (2 ng/ml) than in the presence of a high concentration of EGF (20 ng/ml), whereas the suppression of NPC number by 15d-PGJ_2 was evident even in the presence of a high concentration of EGF (20 ng/ml). To determine whether the regulation of viable cell number by 15d-PGJ_2 is due to an action on cell division, we next examined the effect of 15d-PGJ_2 on DNA synthesis activity of NPCs using a BrdU incorporation assay. We first investigated the time dependency of BrdU incorporation to determine the plateau reached after labeling the whole cycling population under our experimental condition. BrdU (1 μM) was added to the culture medium during the last 12 h (36–48 h after EGF stimulation), 24 h (24–48 h), 36 h (12–48 h) or 48 h (0–48 h) of the exposure period, and cells were fixed and processed for BrdU immunocytochemistry. As shown in Supplemental Fig. 2, the

Molecular Pharmacology Fast Forward. Published on January 19, 2010 as DOI: 10.1124/mol.109.061010
This article has not been copyedited and formatted. The final version may differ from this version.

proportion of BrdU-labeled cells increased in EGF concentration- and exposure time-dependent manners and reached a plateau after 36 h of labeling time. The maximum proportion of BrdU-labeled cells (25–33%) was comparable to that reported by another laboratory using the neurosphere method (approximately 40% of BrdU-labeled cells after 16 h of exposure) (Palazuelos et al., 2006), suggesting that the population of cells undergoing cell cycling is around 30–40 % in neurosphere culture conditions. Based on this observation, we adopted the last 12 h of the BrdU-labeling protocol to examine accelerative and/or suppressive potential of 15d-PGJ_2 on the proliferation of NPCs. EGF increased the proportion of BrdU-labeled cells in a concentration-dependent manner (Fig. 1B). In the presence of EGF (2 and 20 ng/ml), 15d-PGJ_2 at a low concentration (0.3 μM) significantly increased the amount of BrdU incorporation, whereas at a high concentration (over 0.5 μM) it significantly suppressed the amount of BrdU incorporation (Fig. 1B).

The effect of 15d-PGJ_2 on the cell death of NPCs. We next investigated whether 15d-PGJ_2 induced cell death using TUNEL staining, which enabled us to detect apoptosis-associated DNA strand breaks (Gavrieli et al., 1992). As shown in Figure 2, the proportion of TUNEL-positive cells in control group was 11.62 ± 5.06%. Treatment

Molecular Pharmacology Fast Forward. Published on January 19, 2010 as DOI: 10.1124/mol.109.061010
This article has not been copyedited and formatted. The final version may differ from this version.

with 15d-PGJ_2 at high concentrations (1–10 μM) caused an approximately 3.8–5.4-fold increase in the proportion of TUNEL-positive cells, while low concentrations (0.01–0.3 μM) of 15d-PGJ_2 failed to affect this proportion. Similarly, PGD_2 at high concentrations (3–10 μM) significantly increased the proportion of TUNEL-positive cells (Supplemental Fig. 3). We noticed that the proportion of TUNEL-positive cells induced by 15d-PGJ_2 was greater than by that induced by PGD_2.

The effect of 15d-PGJ_2 on the multipotency of cultured NPCs. Because NPCs are known to differentiate into neural and glial cells in the absence of growth factor, we examined the effect of 15d-PGJ_2 on the multipotency of cultured NPCs using immunocytochemistry with antibodies to neuronal (Tuj1) or astroglial (GFAP) markers. There were no significant changes in the proportions of Tuj1-positive and GFAP-positive cells after treatment with 15d-PGJ_2 at the examined concentrations (0.3–0.5 μM) (Fig. 3). Treatment with 1 μM 15d-PGJ_2 caused abundant cell death in the absence of EGF (data not shown).

The effect of PPARγ antagonist on the action of 15d-PGJ_2 on the proliferation of NPCs. Because 15d-PGJ_2 is known to act as a natural ligand for PPARγ, we next

Molecular Pharmacology Fast Forward. Published on January 19, 2010 as DOI: 10.1124/mol.109.061010
This article has not been copyedited and formatted. The final version may differ from this version.

examined the effect of the PPARγ irreversible antagonist GW9662 on the regulation of proliferation by 15d-PGJ_2 using the WST-8 assay. GW9662 alone did not affect basal or EGF-induced proliferation in the absence of 15d-PGJ_2 (Fig. 4). Even in the presence of GW9662 (0.1 μM), 15d-PGJ_2 at low concentrations (around 0.3 μM) facilitated EGF-induced proliferation of NPCs, whereas at high concentrations (1–10 μM) it suppressed EGF-induced proliferation of NPCs (Fig. 4). Pretreatment with GW9662 also failed to affect the suppression of the viable cell number induced by 15d-PGJ_2 at high concentrations (1 and 10 μM) in the absence of EGF. Although it has been reported that GW9662 shows some cell toxicity at concentrations higher than 1 μM (Ray et al., 2006), the biphasic actions of 15d-PGJ_2 on EGF-induced proliferation of NPCs were still observed in the presence of a high concentration of GW9662 (10 μM) (data not shown). In the same way, we investigated the effects of GW9662 on the regulation of proliferation by PGD_2 (Supplemental Fig. 4). Although there were some significant differences between vehicle and GW9662 groups at some concentrations of PGD_2, (3 μM in the absence of EGF, 2 and 3 μM in the presence of 2 ng/ml EGF and 1, 2 and 3 μM in the presence of 20 ng/ml EGF, $p < 0.05$, Student's *t*-test, significant marks not shown in figure), the biphasic actions of PGD_2 on proliferation of NPCs were still observed in the GW9662-treated group (Supplemental Fig. 4).

Molecular Pharmacology Fast Forward. Published on January 19, 2010 as DOI: 10.1124/mol.109.061010
This article has not been copyedited and formatted. The final version may differ from this version.

The effect of CAY10410 on EGF-induced proliferation of NPCs. To investigate whether the electrophilic property of 15d-PGJ_2 is necessary for its action, we examined the effect of CAY10410 (9,10-dehydro-15-deoxy-$\Delta^{12,14}$-prostaglandin J_2), a structural analog of 15d-PGJ_2 with PPARγ agonistic activity but lacking the electrophilic carbon at position 9 in the cyclopentenone ring (Ray et al., 2006). We found that CAY10410 at concentrations up to 1 μM failed to influence EGF-induced proliferation of NPCs (Fig. 5). However, CAY10410 at 10 μM significantly increased the viable cell number in the presence of 2 ng/ml EGF. These results suggest that the electrophilic carbon at position 9 in 15d-PGJ_2 is critical for its biphasic effects on the proliferation of NPCs.

The effect of 15d-PGJ_2 on ROS levels in NPCs. Because PPARγ was not significantly involved in the regulation of the proliferation by 15d-PGJ_2, we further investigated the mechanisms underlying such regulation by 15d-PGJ_2. It has been reported that the intracellular ROS levels in SH-SY5Y cells were elevated by 15d-PGJ_2 in a concentration-dependent manner (Shibata et al., 2003). To determine whether 15d-PGJ_2 affects ROS levels in NPCs, we used a ROS-detecting probe, H_2DCFDA. This cell permeable indicator is nonfluorescent and contains acetate groups that can be

Molecular Pharmacology Fast Forward. Published on January 19, 2010 as DOI: 10.1124/mol.109.061010
This article has not been copyedited and formatted. The final version may differ from this version.

hydrolyzed by intracellular esterase, which enables it to react with oxidants to generate detectable fluorescence (Hempel et al., 1999; Ray et al., 2006). As shown in Fig. 6, 15d-PGJ_2 increased the proportion of H_2DCFDA-fluorescence-positive cells as well as the level of fluorescence intensity per cell in a concentration-dependent manner, indicating that 15d-PGJ_2 elevated intracellular ROS levels. By contrast, CAY10410 failed to affect the intracellular ROS level at concentrations of up to 1 μM. Furthermore, pretreatment with GSH-EE, a membrane-permeable analogue of the endogenous antioxidant glutathione, suppressed the increase in ROS level induced by 15d-PGJ_2. Phorbol ester PMA, used as a positive control reagent, also increased the ROS level in NPCs.

The effects of 15d-PGJ_2 on endogenous GSH levels and the effect of GSH-EE treatment on the regulation of proliferation by 15d-PGJ_2. Because it has been reported that 15d-PGJ_2 binds covalently to endogenous GSH and decreases its intracellular level, we examined the effects of 15d-PGJ_2 on the intracellular GSH level in NPCs. The level of total intracellular GSH (both reduced and oxidized forms) was measured 12 h after exposure to 15d-PGJ_2. As shown in Fig. 7A, 15d-PGJ_2 at 0.3 μM did not change the GSH level; however, 15d-PGJ_2 at concentrations of 0.5, 1 and 10 μM

Molecular Pharmacology Fast Forward. Published on January 19, 2010 as DOI: 10.1124/mol.109.061010
This article has not been copyedited and formatted. The final version may differ from this version.

significantly decreased the level of GSH to 50–60% of the level in the vehicle group.

If the decrease in GSH levels followed by ROS elevation is indispensable for the biphasic action of 15d-PGJ_2, treatment with an antioxidant such as GSH would reverse the effects of 15d-PGJ_2 on the proliferation of NPCs. To test this hypothesis, we next investigated whether supplementation with GSH-EE could prevent the effects of 15d-PGJ_2 on the proliferation of NPCs using WST-8 assay. NPCs were pretreated with GSH-EE (2 mM) for 1 h and then treated with or without various concentrations of 15d-PGJ_2 (0.01–10 μM) in the presence of EGF (2, 20 ng/ml) for 48 h. In the presence of a low concentration of EGF (2 ng/ml), treatment with GSH-EE prevented the facilitatory actions of 0.1 and 0.3 μM 15d-PGJ_2 and the inhibitory actions of 0.5, 1 and 10 μM 15d-PGJ_2 (Fig. 7B). Similarly, in the presence of a high concentration of EGF (20 ng/ml), GSH-EE suppressed the facilitatory and inhibitory effects of 15d-PGJ_2 (Fig. 7B). Similar to these effects on 15d-PGJ_2 actions, pretreatment with GSH-EE (2 mM) also blunted the regulation of NPC proliferation by PGD_2 (Supplemental Fig. 5). These results suggest that glutathione plays an important role in the actions of 15d-PGJ_2.

Effect of central injection of 15d-PGJ_2 on the proliferation of NPCs located in the DG of postnatal mice. To substantiate the relevance of our *in vitro* observations, we

Molecular Pharmacology Fast Forward. Published on January 19, 2010 as DOI: 10.1124/mol.109.061010
This article has not been copyedited and formatted. The final version may differ from this version.

next examined the effect of various doses of 15d-PGJ_2 (0.3–30 ng) on the proliferation of neural stem/progenitor cells in the DG *in vivo* using BrdU immunohistochemistry. Mice were given BrdU (50 mg/kg i.p.) 5 h or 24 h after 15d-PGJ_2 injection to investigate the acute and subchronic effects of 15d-PGJ_2, respectively. When BrdU was injected 5 h after 15d-PGJ_2, the number of BrdU-labeled cells in the DG was significantly decreased only by highest dose of 15d-PGJ_2 (30 ng) (Fig. 8A). By contrast, when BrdU was injected 24 h after 15d-PGJ_2, 15d-PGJ_2 at a low dose (1 ng) significantly increased the number of BrdU-labeled cells to 148% of the level in the control group, while 15d-PGJ_2 at a high dose (30 ng) decreased the number of BrdU-labeled cells to 71% of the level in the control group (Fig. 8A, 8B). These results suggest that 15d-PGJ_2 biphasically regulates the proliferation of neural stem/progenitor cells in the DG of postnatal mice *in vivo*.

Molecular Pharmacology Fast Forward. Published on January 19, 2010 as DOI: 10.1124/mol.109.061010
This article has not been copyedited and formatted. The final version may differ from this version.

Discussion

In the present study, we examined the mode of action of 15d-PGJ_2 on the proliferation of mouse hippocampal NPCs *in vitro* and *in vivo*. Using assays assessing the relative viable cell number as well as DNA synthesis activity, we found that 15d-PGJ_2 showed biphasic effects on the EGF-induced proliferation of NPCs; facilitation at low concentrations (around 0.3 μM) and suppression at higher concentrations (0.5–10 μM) *in vitro*. GW9662, an inhibitor of PPARγ, failed to abolish the effects of 15d-PGJ_2. We also found that the electrophilic carbon at position 9 is critical for the action of 15d-PGJ_2 on proliferation, because CAY10410, a structural analog of 15d-PGJ_2 lacking the electrophilic carbon, did not show 15d-PGJ_2-like actions. Treatment with 15d-PGJ_2 at low or high concentrations increased ROS levels and decreased endogenous GSH levels. Furthermore, supplementation with GSH-EE (2 mM) diminished the biphasic effects of 15d-PGJ_2. Finally, similar biphasic effects of 15d-PGJ_2, facilitation at low dose and suppression at high dose, were observed in the dentate gyri of postnatal mice *in vivo*.

15d-PGJ_2 contains a reactive electrophilic carbon in the cyclopentenone ring and changes the redox state by covalently modifying cysteine residues in their target proteins (Rossi et al., 2000; Straus et al., 2000). We previously reported that MCI-186,

Molecular Pharmacology Fast Forward. Published on January 19, 2010 as DOI: 10.1124/mol.109.061010
This article has not been copyedited and formatted. The final version may differ from this version.

which is known as an antioxidant, suppressed EGF-induced proliferation of NPCs derived from mouse ganglionic eminence and increased subsequent neural differentiation (Moriya et al., 2007). Moreover, it has been reported that the level of ROS is significantly higher in neural precursor cells compared with other primary and transformed cell lines and would be drastically changed by cell density (Limoli et al., 2004). These authors demonstrated that ROS levels were significantly elevated under low-density conditions when compared with high-density conditions and higher ROS levels found at lower cell densities were associated with elevated proliferation (Limoli et al., 2004). These lines of evidence suggest that the cellular redox state plays important roles in regulating the proliferative activity of NPCs. In the present study, we found that 15d-PGJ_2 increased ROS levels and that supplementation with GSH-EE partially suppressed the effects of 15d-PGJ_2 on the proliferative activity of NPCs. At higher concentrations (1–10 μM), 15d-PGJ_2 decreases the amount of GSH probably by covalently scavenging intracellular GSH, and strongly increases cellular oxidation over the physiological ranges, resulting in cell cycle arrest followed by apoptosis of NPCs. Similarly, 15d-PGJ_2 at high concentrations (5–20 μM) was reported to induce apoptosis in human B lymphocytes by increasing intracellular ROS levels in a PPARγ-independent manner (Ray et al., 2006). Taken together, these findings suggest

Molecular Pharmacology Fast Forward. Published on January 19, 2010 as DOI: 10.1124/mol.109.061010
This article has not been copyedited and formatted. The final version may differ from this version.

that 15d-PGJ_2 extraordinarily increases intracellular ROS levels and subsequently causes cytotoxicity by inducing cellular oxidative stress.

On the other hand, 15d-PGJ_2 at a lower concentration (0.3 μM) failed to influence the amount of GSH, but modestly increased the intracellular ROS level; this was associated with the facilitation of NPC proliferation. The mechanism underlying the GSH-independent increase in ROS levels elicited by low concentrations of 15d-PGJ_2 is not clear at present. We speculate that redox-related substances other than GSH may be involved in the effects of a low concentration of 15d-PGJ_2. For example, thioredoxin (Trx), an important redox regulatory molecule, is reported to be a target protein of 15d-PGJ_2 (Shibata et al., 2003). 15d-PGJ_2 covalently modifies cysteine residues and inhibits the activity of Trx, which has a role in removing intracellular ROS, leading the rupture of intracellular redox state. Because supplementation with GSH-EE partly suppressed the effects of 15d-PGJ_2 on the self-renewal ability of NPCs, 15d-PGJ_2 can covalently modify other redox regulatory molecules, such as Trx. Also, the signaling pathways downstream of ROS elevation, involved in 15d-PGJ_2 actions, are not clear at present. It has been reported that H_2O_2, a ROS, rapidly activated the NF-κB pathway in a human T cell line (Schreck et al., 1991). Schreck et al. demonstrated that reactive oxygen directly or indirectly released the inhibitory subunit IκB from NF-κB (Schreck

Molecular Pharmacology Fast Forward. Published on January 19, 2010 as DOI: 10.1124/mol.109.061010
This article has not been copyedited and formatted. The final version may differ from this version.

et al., 1991). To elucidate the signaling molecule(s) mediating 15d-PGJ_2-induced ROS elevation, further experiments will be required.

15d-PGJ_2 has been identified as a natural ligand for PPARγ, which belongs to the nuclear receptor superfamily. It has been reported that 15d-PGJ_2 causes the differentiation of adipocytes via the activation of PPARγ (Forman et al., 1995). On the other hand, in the human leukemia cell line THP-1, 15d-PGJ_2 had biphasic effects on proliferation in a PPARγ-independent manner (Azuma et al., 2004) similar to our present observation. As shown in Figure 5, CAY10410 only at 10 μM increased the viable cell number in the presence of 2 ng/ml EGF. It has been reported that CAY10410, a structural analog of 15d-PGJ_2, lacks the electrophilic carbon at position 9, but shows PPARγ agonistic activity (Shiraki et al., 2005). These authors showed that CAY10410 at 10 μM could act as an agonist of PPARγ; however, it did not react with PPARγ at concentrations lower than 1 μM. Taken together, these findings suggest that PPARγ may be involved in the facilitatory effects of CAY10410 at 10 μM on the proliferation of NPCs in our study.

The DG of the hippocampus is one of two neurogenesis-rich regions in the adult mammalian brain (Altman and Das, 1965; Dayer et al., 2003). We examined whether 15d-PGJ_2 influenced the proliferative activity of neural stem/progenitor cells in the

Molecular Pharmacology Fast Forward. Published on January 19, 2010 as DOI: 10.1124/mol.109.061010
This article has not been copyedited and formatted. The final version may differ from this version.

mouse DG *in vivo*. We observed that intracerebroventricular injection of 30 ng of 15d-PGJ_2 significantly decreased the number of BrdU-labeled cells in the DG, when BrdU was administered 5 h or 24 h after 15d-PGJ_2 injection, suggesting that the suppressive or toxic effects of 15d-PGJ_2 appear acutely. By contrast, the increase in the number of BrdU-labeled cells induced by a low dose of 15d-PGJ_2 was observed only when BrdU was administered 24 h after 15d-PGJ_2 injection, but not when administered 5 h after, suggesting that the facilitating action of 15d-PGJ_2 requires a long period for action (at least 24 h). Furthermore, the difference in the time for the appearance of 15d-PGJ_2 effects between facilitation and suppression implies that the biphasic action of 15d-PGJ_2 may involve different intracellular mechanisms.

There is growing evidence indicating that neurogenesis in adulthood is influenced by certain types of the central diseases such as neuroinflammation. We have previously shown that lipopolysaccharide (LPS) impairs the survival of newly generated cells derived from neural stem/progenitor cells in the DG *in vivo* and these effects of LPS were presumably mediated by cyclooxygenase-2 (COX-2) expression in the DG (Bastos et al., 2008). Interestingly, the central infusion of LPS drastically increases the brain levels of PGD_2, a major metabolite of arachidonic acid in the CNS (Rosenberger et al., 2004). Because the doses of 15d-PGJ_2 used in this study were considered to induce

Molecular Pharmacology Fast Forward. Published on January 19, 2010 as DOI: 10.1124/mol.109.061010
This article has not been copyedited and formatted. The final version may differ from this version.

situation like intracerebral hemorrhage (Zhao et al., 2006), PGD_2, as well as its metabolite 15d-PGJ_2, is a feasible candidate molecule regulating neurogenesis under pathophysiological conditions such as neuroinflammation.

In conclusion, the present study shows that 15d-PGJ_2 exhibits a novel regulation of the proliferation of NPCs and supplementation with GSH prevents the effects of 15d-PGJ_2. Our pharmacological and biochemical analyses show that ROS elevation accompanied with or without depletion of endogenous GSH levels might mediate the facilitatory and inhibitory actions of 15d-PGJ_2. Further experiments will be required to clarify the downstream signaling pathways underlying the regulation of NPC proliferation by 15d-PGJ_2.

References

Altman J and Das GD (1965) Autoradiographic and histological evidence of postnatal hippocampal neurogenesis in rats. *J Comp Neurol* **124**(3):319-335.

Azuma Y, Watanabe K, Date M, Daito M and Ohura K (2004) Possible involvement of p38 in mechanisms underlying acceleration of proliferation by 15-deoxy-Delta(12,14)-prostaglandin J2 and the precursors in leukemia cell line THP-1. *J Pharmacol Sci* **94**(3):261-270.

Bastos GN, Moriya T, Inui F, Katura T and Nakahata N (2008) Involvement of cyclooxygenase-2 in lipopolysaccharide-induced impairment of the newborn cell survival in the adult mouse dentate gyrus. *Neuroscience* **155**(2):454-462.

Dayer AG, Ford AA, Cleaver KM, Yassaee M and Cameron HA (2003) Short-term and long-term survival of new neurons in the rat dentate gyrus. *J Comp Neurol* **460**(4):563-572.

Debril MB, Renaud JP, Fajas L and Auwerx J (2001) The pleiotropic functions of peroxisome proliferator-activated receptor gamma. *J Mol Med* **79**(1):30-47.

Eriksson PS, Perfilieva E, Bjork-Eriksson T, Alborn AM, Nordborg C, Peterson DA and Gage FH (1998) Neurogenesis in the adult human hippocampus. *Nat Med* **4**(11):1313-1317.

Forman BM, Tontonoz P, Chen J, Brun RP, Spiegelman BM and Evans RM (1995) 15-Deoxy-delta 12, 14-prostaglandin J2 is a ligand for the adipocyte determination factor PPAR gamma. *Cell* **83**(5):803-812.

Gage FH (2000) Mammalian neural stem cells. *Science* **287**(5457):1433-1438.

Gavrieli Y, Sherman Y and Ben-Sasson SA (1992) Identification of programmed cell death in situ via specific labeling of nuclear DNA fragmentation. *J Cell Biol* **119**(3):493-501.

Guzman-Marin R, Suntsova N, Stewart DR, Gong H, Szymusiak R and McGinty D (2003) Sleep deprivation reduces proliferation of cells in the dentate gyrus of the hippocampus in rats. *J Physiol* **549**(Pt 2):563-571.

Hayaishi O (2002) Molecular genetic studies on sleep-wake regulation, with special emphasis on the prostaglandin D(2) system. *J Appl Physiol* **92**(2):863-868.

Hempel SL, Buettner GR, O'Malley YQ, Wessels DA and Flaherty DM (1999) Dihydrofluorescein diacetate is superior for detecting intracellular oxidants: comparison with 2',7'-dichlorodihydrofluorescein diacetate, 5(and 6)-carboxy-2',7'-dichlorodihydrofluorescein diacetate, and dihydrorhodamine 123. *Free Radic Biol Med* **27**(1-2):146-159.

Herlong JL and Scott TR (2006) Positioning prostanoids of the D and J series in the

immunopathogenic scheme. *Immunol Lett* **102**(2):121-131.

Huang ZL, Urade Y and Hayaishi O (2007) Prostaglandins and adenosine in the regulation of sleep and wakefulness. *Curr Opin Pharmacol* **7**(1):33-38.

Jiang W, Zhang Y, Xiao L, Van Cleemput J, Ji SP, Bai G and Zhang X (2005) Cannabinoids promote embryonic and adult hippocampus neurogenesis and produce anxiolytic- and antidepressant-like effects. *J Clin Invest* **115**(11):3104-3116.

Kanemura Y, Mori H, Kobayashi S, Islam O, Kodama E, Yamamoto A, Nakanishi Y, Arita N, Yamasaki M, Okano H, Hara M and Miyake J (2002) Evaluation of in vitro proliferative activity of human fetal neural stem/progenitor cells using indirect measurements of viable cells based on cellular metabolic activity. *J Neurosci Res* **69**(6):869-879.

Limoli CL, Rola R, Giedzinski E, Mantha S, Huang TT and Fike JR (2004) Cell-density-dependent regulation of neural precursor cell function. *Proc Natl Acad Sci U S A* **101**(45):16052-16057.

Miller FD and Gauthier AS (2007) Timing is everything: making neurons versus glia in the developing cortex. *Neuron* **54**(3):357-369.

Moriya T, Horie N, Mitome M and Shinohara K (2007) Melatonin influences the

proliferative and differentiative activity of neural stem cells. *J Pineal Res* **42**(4):411-418.

Nakatomi H, Kuriu T, Okabe S, Yamamoto S, Hatano O, Kawahara N, Tamura A, Kirino T and Nakafuku M (2002) Regeneration of hippocampal pyramidal neurons after ischemic brain injury by recruitment of endogenous neural progenitors. *Cell* **110**(4):429-441.

Ogorochi T, Narumiya S, Mizuno N, Yamashita K, Miyazaki H and Hayaishi O (1984) Regional distribution of prostaglandins D2, E2, and F2 alpha and related enzymes in postmortem human brain. *J Neurochem* **43**(1):71-82.

Oliva JL, Perez-Sala D, Castrillo A, Martinez N, Canada FJ, Bosca L and Rojas JM (2003) The cyclopentenone 15-deoxy-delta 12,14-prostaglandin J2 binds to and activates H-Ras. *Proc Natl Acad Sci U S A* **100**(8):4772-4777.

Palazuelos J, Aguado T, Egia A, Mechoulam R, Guzman M and Galve-Roperh I (2006) Non-psychoactive CB2 cannabinoid agonists stimulate neural progenitor proliferation. *Faseb J* **20**(13):2405-2407.

Parent JM, Yu TW, Leibowitz RT, Geschwind DH, Sloviter RS and Lowenstein DH (1997) Dentate granule cell neurogenesis is increased by seizures and contributes to aberrant network reorganization in the adult rat hippocampus. *J*

Neurosci **17**(10):3727-3738.

Ray DM, Akbiyik F and Phipps RP (2006) The peroxisome proliferator-activated receptor gamma (PPARgamma) ligands 15-deoxy-Delta12,14-prostaglandin J2 and ciglitazone induce human B lymphocyte and B cell lymphoma apoptosis by PPARgamma-independent mechanisms. *J Immunol* **177**(8):5068-5076.

Reynolds BA, Tetzlaff W and Weiss S (1992) A multipotent EGF-responsive striatal embryonic progenitor cell produces neurons and astrocytes. *J Neurosci* **12**(11):4565-4574.

Rosenberger TA, Villacreses NE, Hovda JT, Bosetti F, Weerasinghe G, Wine RN, Harry GJ and Rapoport SI (2004) Rat brain arachidonic acid metabolism is increased by a 6-day intracerebral ventricular infusion of bacterial lipopolysaccharide. *J Neurochem* **88**(5):1168-1178.

Rossi A, Kapahi P, Natoli G, Takahashi T, Chen Y, Karin M and Santoro MG (2000) Anti-inflammatory cyclopentenone prostaglandins are direct inhibitors of IkappaB kinase. *Nature* **403**(6765):103-108.

Schreck R, Rieber P and Baeuerle PA (1991) Reactive oxygen intermediates as apparently widely used messengers in the activation of the NF-kappa B transcription factor and HIV-1. *Embo J* **10**(8):2247-2258.

Shibata T, Kondo M, Osawa T, Shibata N, Kobayashi M and Uchida K (2002) 15-deoxy-delta 12,14-prostaglandin J2. A prostaglandin D2 metabolite generated during inflammatory processes. *J Biol Chem* **277**(12):10459-10466.

Shibata T, Yamada T, Ishii T, Kumazawa S, Nakamura H, Masutani H, Yodoi J and Uchida K (2003) Thioredoxin as a molecular target of cyclopentenone prostaglandins. *J Biol Chem* **278**(28):26046-26054.

Shiraki T, Kamiya N, Shiki S, Kodama TS, Kakizuka A and Jingami H (2005) Alpha,beta-unsaturated ketone is a core moiety of natural ligands for covalent binding to peroxisome proliferator-activated receptor gamma. *J Biol Chem* **280**(14):14145-14153.

Smith WL (1989) The eicosanoids and their biochemical mechanisms of action. *Biochem J* **259**(2):315-324.

Smith WL (1992) Prostanoid biosynthesis and mechanisms of action. *Am J Physiol* **263**(2 Pt 2):F181-191.

Straus DS, Pascual G, Li M, Welch JS, Ricote M, Hsiang CH, Sengchanthalangsy LL, Ghosh G and Glass CK (2000) 15-deoxy-delta 12,14-prostaglandin J2 inhibits multiple steps in the NF-kappa B signaling pathway. *Proc Natl Acad Sci U S A* **97**(9):4844-4849.

Tropepe V, Sibilia M, Ciruna BG, Rossant J, Wagner EF and van der Kooy D (1999) Distinct neural stem cells proliferate in response to EGF and FGF in the developing mouse telencephalon. *Dev Biol* **208**(1):166-188.

Uchida K, Kumihashi K, Kurosawa S, Kobayashi T, Itoi K and Machida T (2002) Stimulatory effects of prostaglandin E2 on neurogenesis in the dentate gyrus of the adult rat. *Zoolog Sci* **19**(11):1211-1216.

Walczak R and Tontonoz P (2002) PPARadigms and PPARadoxes: expanding roles for PPARgamma in the control of lipid metabolism. *J Lipid Res* **43**(2):177-186.

Weiss S, Reynolds BA, Vescovi AL, Morshead C, Craig CG and van der Kooy D (1996) Is there a neural stem cell in the mammalian forebrain? *Trends Neurosci* **19**(9):387-393.

Zhao X, Zhang Y, Strong R, Grotta JC and Aronowski J (2006) 15d-Prostaglandin J2 activates peroxisome proliferator-activated receptor-gamma, promotes expression of catalase, and reduces inflammation, behavioral dysfunction, and neuronal loss after intracerebral hemorrhage in rats. *J Cereb Blood Flow Metab* **26**(6):811-820.

Footnotes

This work was supported by a Grant-in-Aid for Scientific Research on Priority Areas-Molecular Brain Science-from the Ministry of Education, Culture, Sports, Science and Technology of Japan (20022002).

Molecular Pharmacology Fast Forward. Published on January 19, 2010 as DOI: 10.1124/mol.109.061010
This article has not been copyedited and formatted. The final version may differ from this version.

Figure legends

Fig. 1. The effect of 15d-PGJ_2 on EGF-induced proliferation of cultured NPCs. Dispersed NPCs from primary neurospheres were seeded in non-treatment 96-well plates at a density of 1×10^5 cells/ml and cultured for 12 h in the absence of EGF. Subsequently, they were treated with or without various concentrations of 15d-PGJ_2 (0.01–10 μM) in the presence or absence of EGF (0, 2, 20 ng/ml) for 48 h. The number of viable cells and the DNA synthesis activity were assessed by WST-8 assay (A) and BrdU incorporation assay (B), respectively. (A) In the WST-8 assay, WST-8 solution was added to each well and incubated for an additional 5 h. The value of the vehicle group in the presence of 20 ng/ml EGF was set to 100%. The data are means ± S.E.M. of four to six wells. *; significant difference from vehicle control in each concentration of EGF ($p < 0.05$, One-way ANOVA followed by Dunnett's test). (B) In the BrdU incorporation assay, cells were labeled with BrdU (1 μM) 12 h prior to fixation and BrdU-labeled cells were stained by immunocytochemistry. Representative images (a) and the proportion of BrdU-labeled cells among all cells (b) are shown. The data are means ± S.E.M. of four to five wells. *; significant difference from vehicle control in each concentration of EGF ($p < 0.05$, One-way ANOVA followed by Dunnett's test). Scale bar = 200 μm.

Molecular Pharmacology Fast Forward. Published on January 19, 2010 as DOI: 10.1124/mol.109.061010
This article has not been copyedited and formatted. The final version may differ from this version.

Fig. 2. The effect of 15d-PGJ_2 on the cell death of NPCs. Dispersed NPCs from primary neurospheres were seeded in LAB-Tek® chamber Slides pre-coated with poly-L-lysine followed by laminin, at a density of 4 x 10^5 cells/ml and cultured for 12 h in the absence of EGF. Subsequently, they were treated with or without various concentrations of 15d-PGJ_2 (0.01–10 μM) in the presence of EGF (2 ng/ml) for 48 h. After cells were fixed with PFA, the dead cells were visualized by TUNEL staining. Representative images (A) and the proportion of TUNEL (+)-cells (B) are shown. The data are means ± S.E.M. of three wells. *; significant difference from vehicle control ($p < 0.05$, One-way ANOVA followed by Dunnett's test). Scale bar = 200 μm.

Fig. 3. The effect of 15d-PGJ_2 on the multipotency of cultured NPCs. NPCs were treated with or without various concentrations of 15d-PGJ_2 in the absence of EGF for 96 h. Differentiation was evaluated by fluorescence-based immunocytochemistry using a mouse monoclonal antibody against Tuj1 (green), a neural marker, a rabbit polyclonal antibody against GFAP (red), an astroglial marker, and Hoechst 33258 (blue). Representative immunofluorescence images (A) and the proportion of Tuj1 (+)-cells (left) and GFAP (+)-cells (right) (B) are shown. The data are means ± S.E.M. of four

Molecular Pharmacology Fast Forward. Published on January 19, 2010 as DOI: 10.1124/mol.109.061010
This article has not been copyedited and formatted. The final version may differ from this version.

wells. Scale bar = 50 μm.

Fig. 4. The effect of PPARγ antagonist on the regulation of NPC proliferation by 15d-PGJ_2. Dispersed NPCs from primary neurospheres were seeded in non-treatment 96-well plates at a density of 1 x 10^5 cells/ml and cultured for 12 h in the absence of EGF. After pretreatment with or without PPARγ antagonist, GW9662 (0.1 μM), for 1 h, cells were stimulated with or without various concentrations of 15d-PGJ_2 (0.01–10 μM) in the presence or absence of EGF (0, 2, 20 ng/ml) for 48 h. The number of viable cells was assessed by WST-8 assay. The value of control group was set to 100%. The data are means ± S.E.M. of three to four wells. *; significant difference from 15d-PGJ_2-free (0 μM) in vehicle group, $^{\#}$; significant difference from 15d-PGJ_2-free (0 μM) in GW9662 group ($p < 0.05$, One-way ANOVA followed by Dunnett's test). Note that there was no significant difference between the vehicle and GW9662 groups.

Fig. 5. The effect of CAY10410 on EGF-induced proliferation of NPCs. The details are the same as those in Fig. 1 legend. The value of the vehicle group at 20 ng/ml EGF was set to 100%. The data are means ± S.E.M. of three to four wells. *; significant difference from the vehicle control in 2 ng/ml EGF group ($p < 0.05$, One-way ANOVA

Molecular Pharmacology Fast Forward. Published on January 19, 2010 as DOI: 10.1124/mol.109.061010
This article has not been copyedited and formatted. The final version may differ from this version.

followed by Dunnett's test).

Fig. 6. The effect of 15d-PGJ_2 on ROS levels in NPCs. After incubation in the absence of EGF for 12 h, NPCs were treated with or without various concentrations of 15d-PGJ_2, GSH-EE, CAY10410 or PMA in the presence of EGF (2 ng/ml) for 2 h. Immediately after the loading of H_2DCFDA (10 μM) during the last 30 min of the incubation period, cells were washed with MHM and fluorescent images were obtained using a fluorescence microscope (A). The proportion of positive cells (a) and the level of fluorescence intensity per cell (b) were calculated by Scion® Image (B). The data are means ± S.E.M. of three to six wells (a) or 65–312 cells. *; significant difference from the vehicle control ($p < 0.05$, One-way ANOVA followed by Fisher's PLSD test). Scale bar = 200 μm.

Fig. 7. The effect of 15d-PGJ_2 on the intracellular GSH level (A). NPCs were treated with or without various concentrations of 15d-PGJ_2 in the presence of EGF (2 ng/ml) for 12 h and the total GSH level was measured using enzymatic reducing cycle system. The data are means ± S.E.M. of four experiments. *; significant difference from vehicle control ($p < 0.05$, One-way ANOVA followed by Dunnett's test). (B) The effect

Molecular Pharmacology Fast Forward. Published on January 19, 2010 as DOI: 10.1124/mol.109.061010
This article has not been copyedited and formatted. The final version may differ from this version.

of pretreatment with GSH-EE on the regulation of the NPC proliferation by 15d-PGJ_2. The details are same as those in Fig. 4 legend. The value of the control group was set to 100%. The data are means ± S.E.M. of three to four wells. $^{\#}$; significant difference from 15d-PGJ_2-free (0 μM) in the vehicle group, †; significant difference from 15d-PGJ_2-free (0 μM) in the GSH-EE group ($p < 0.05$, One-way ANOVA followed by Dunnett's test). *; significant difference between the vehicle and GSH-EE groups at each concentration of 15d-PGJ_2. ($p < 0.05$, Student's *t*-test).

Fig. 8. The effect of the central injection of 15d-PGJ_2 on the proliferation of neural stem/progenitor cells in the dentate gyrus (DG) of postnatal mice. (A) The number of BrdU-labeled cells in the DG of mice that were given BrdU 5 h after (a) and 24 h after (b) 15d-PGJ_2 injection. Five h (a) or 24 h (b) after i.c.v injection of 15d-PGJ_2 or vehicle, animals were intraperitoneally injected with BrdU (50 mg/kg). Two hours after BrdU injection, animals were sacrificed and coronal brain sections were processed for BrdU immunohistochemistry. The data are means ± S.E.M. of three to five mice. *; significant difference from the vehicle control ($p < 0.05$, Dunnett's test). (B) Representative immunofluorescence images of BrdU-labeled cells in the DG of mice that were given BrdU 24 h after 15d-PGJ_2 or vehicle injection. The dashed rectangles in

Molecular Pharmacology Fast Forward. Published on January 19, 2010 as DOI: 10.1124/mol.109.061010
This article has not been copyedited and formatted. The final version may differ from this version.

the low power image indicate the area shown in the high power image. GCL, granule cell layer; SGZ, subgranular zone. Scale bar = 100 μm.

Figure 1

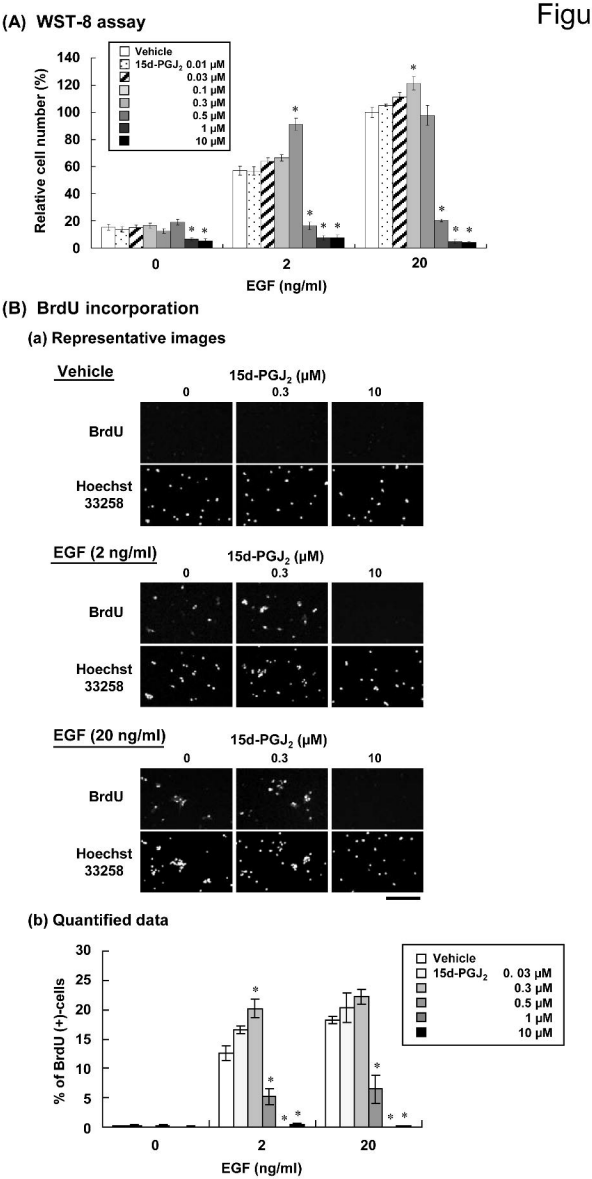
(A) WST-8 assay
Vehicle
15d-PGJ2 0.01 μM
0.03 μM
0.1 μM
0.3 μM
0.5 μM
1 μM
10 μM
Relative cell number (%)
EGF (ng/ml)
(B) BrdU incorporation
(a) Representative images
Vehicle
EGF (2 ng/ml)
EGF (20 ng/ml)
15d-PGJ2 (μM)
BrdU
Hoechst 33258
(b) Quantified data
% of BrdU (+)-cells
Vehicle
15d-PGJ2 0. 03 μM
0.3 μM
0.5 μM
1 μM
10 μM

Figure 2

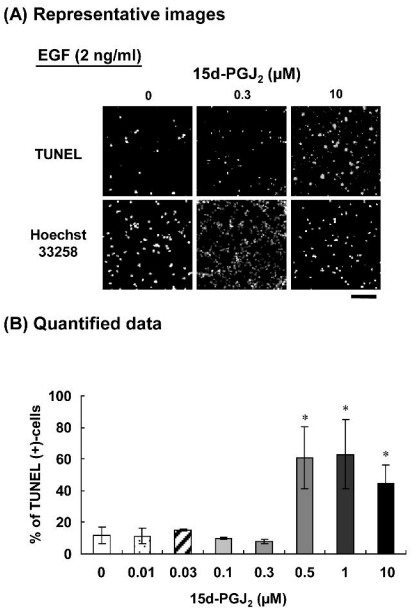
(A) Representative images
EGF (2 ng/ml)
15d-PGJ2 (μM)
0
0.3
10
TUNEL
Hoechst 33258
(B) Quantified data
% of TUNEL (+)-cells
100
80
60
40
20
0
0
0.01
0.03
0.1
0.3
0.5
1
10
15d-PGJ2 (μM)
*
*
*

Figure 3

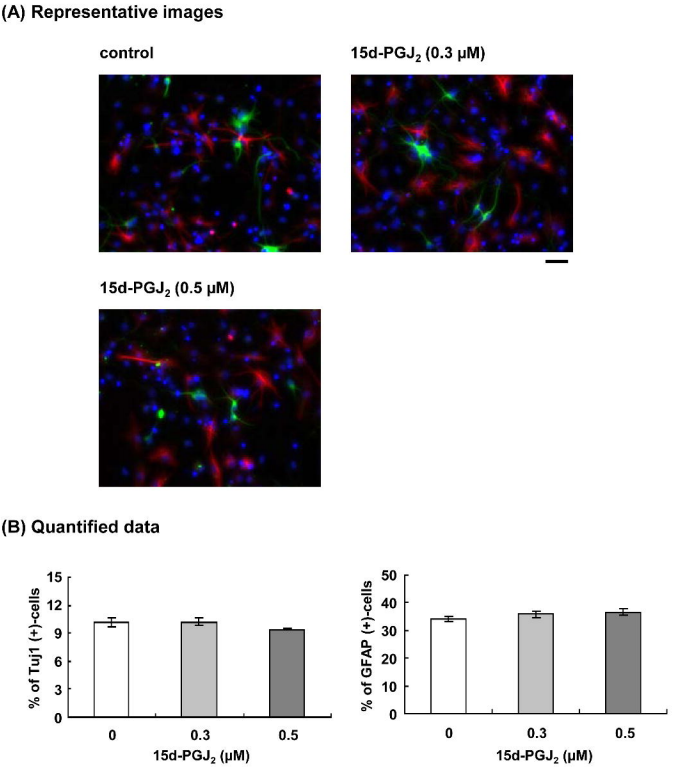
(A) Representative images
control
15d-PGJ2 (0.3 μM)
15d-PGJ2 (0.5 μM)
(B) Quantified data
% of Tuj1 (+)-cells
15
12
9
6
3
0
0
0.3
0.5
15d-PGJ2 (μM)
% of GFAP (+)-cells
50
40
30
20
10
0
0
0.3
0.5
15d-PGJ2 (μM)

Figure 4

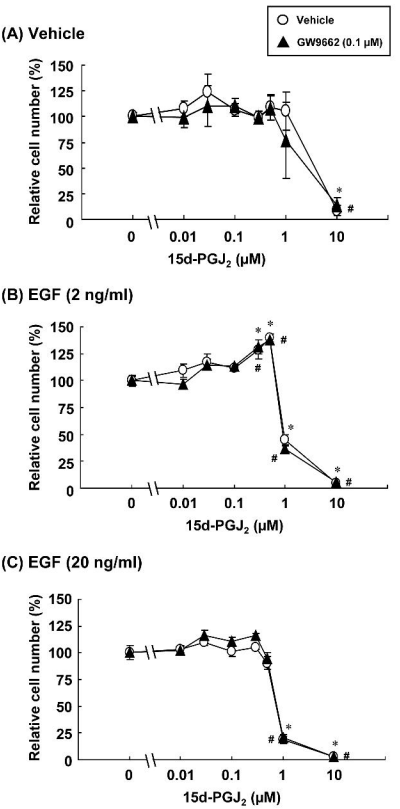
(A) Vehicle
Vehicle
GW9662 (0.1 μM)
Relative cell number (%)
150
125
100
75
50
25
0
0
0.01
0.1
1
10
15d-PGJ2 (μM)
(B) EGF (2 ng/ml)
Relative cell number (%)
15d-PGJ2 (μM)
(C) EGF (20 ng/ml)
Relative cell number (%)
15d-PGJ2 (μM)

Figure 5

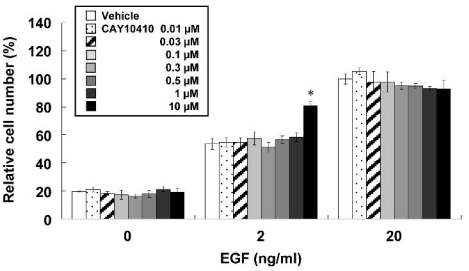
Vehicle
CAY10410 0.01 μM
0.03 μM
0.1 μM
0.3 μM
0.5 μM
1 μM
10 μM
Relative cell number (%)
140
120
100
80
60
40
20
0
*
0
2
20
EGF (ng/ml)

Figure 6

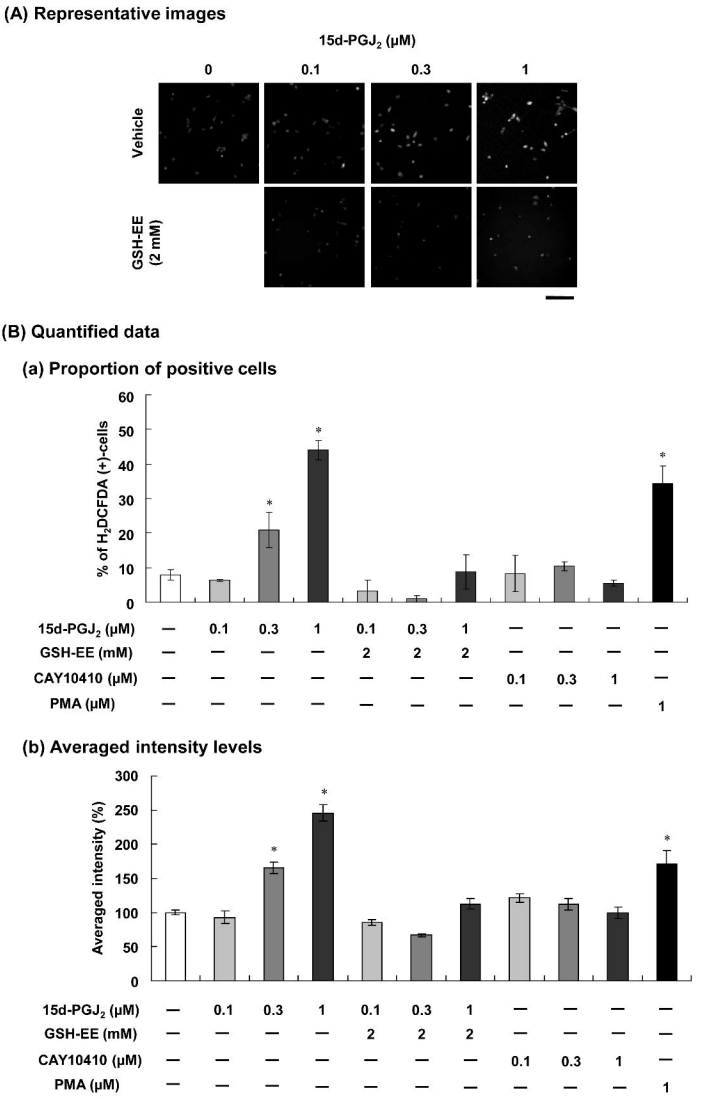
(A) Representative images
15d-PGJ2 (μM)
0
0.1
0.3
1
Vehicle
GSH-EE (2 mM)
(B) Quantified data
(a) Proportion of positive cells
% of H2DCFDA (+)-cells
60
50
40
30
20
10
0
15d-PGJ2 (μM) — 0.1 0.3 1 0.1 0.3 1 — — — —
GSH-EE (mM) — — — — 2 2 2 — — — —
CAY10410 (μM) — — — — — — — 0.1 0.3 1 —
PMA (μM) — — — — — — — — — — 1
(b) Averaged intensity levels
Averaged intensity (%)
300
250
200
150
100
50
0
15d-PGJ2 (μM) — 0.1 0.3 1 0.1 0.3 1 — — — —
GSH-EE (mM) — — — — 2 2 2 — — — —
CAY10410 (μM) — — — — — — — 0.1 0.3 1 —
PMA (μM) — — — — — — — — — — 1

Figure 7

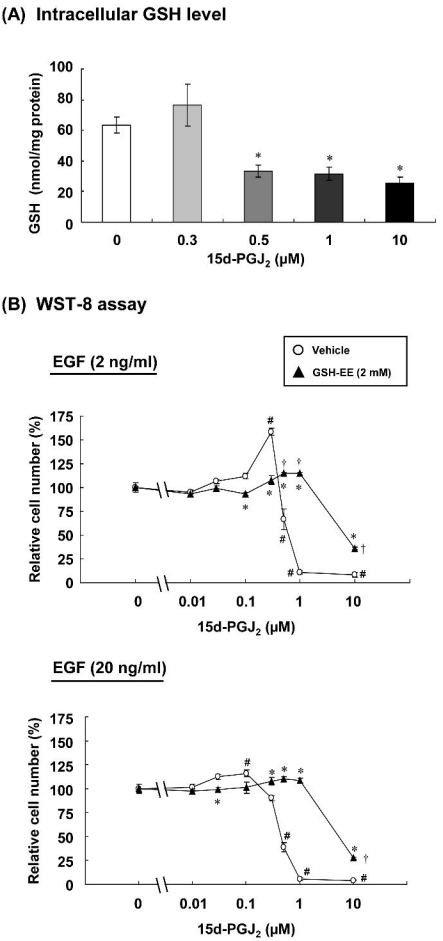
(A) Intracellular GSH level
GSH (nmol/mg protein)
100
80
60
40
20
0
0
0.3
0.5
1
10
15d-PGJ2 (μM)
(B) WST-8 assay
EGF (2 ng/ml)
Vehicle
GSH-EE (2 mM)
Relative cell number (%)
175
150
125
100
75
50
25
0
0
0.01
0.1
1
10
15d-PGJ2 (μM)
EGF (20 ng/ml)
Relative cell number (%)
175
150
125
100
75
50
25
0
0
0.01
0.1
1
10
15d-PGJ2 (μM)

Figure 8

(A) Quantified data

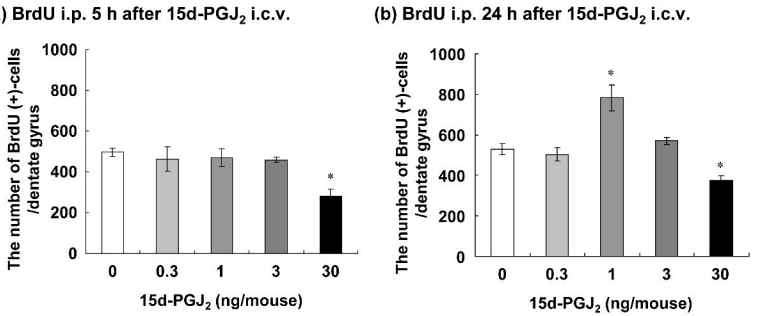

(B) Representative images

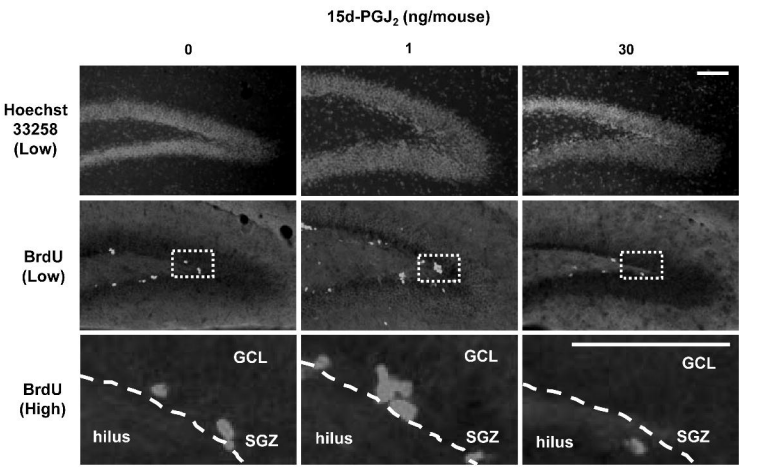

Supplementary data

15-Deoxy-$\Delta^{12,14}$-Prostaglandin J_2 Biphasically Regulates the Proliferation of Mouse Hippocampal Neural Progenitor Cells by Modulating the Redox State

Takashi Katura, Takahiro Moriya, Norimichi Nakahata

Molecular Pharmacology

Supplementary Figure legends

Supplementary Fig. 1. The effects of DP1 and DP2 antagonists on the regulation of NPC proliferation by PGD_2. Dispersed NPCs from the primary neurospheres were seeded in non-treatment 96-well plates at a density of 1×10^5 cells/ml and cultured for 12 h in the absence of EGF. After pretreatment with vehicle, the DP1 antagonist BWA868C (10 μM) or the DP2 antagonist ramatroban (10 μM) (A) for 1 h, cells were stimulated with or without various concentrations of PGD_2 (0.1–10 μM) in the presence or absence of EGF (0, 2, 20 ng/ml) for 48 h. The number of viable cells was assessed by WST-8 assay. The value of the control group was set to 100%. The data are means ± S.E.M. of three to four wells. *, #, †; significant difference from PGD_2-free (0 μM) in the vehicle, BWA868C or ramatroban group, respectively ($p < 0.05$, One-way ANOVA followed by Dunnett's test).

Supplementary Fig. 2. The exposure time dependency for BrdU incorporation in NPCs in the absence or presence of EGF. After incubation in the absence of EGF for 12 h, NPCs were stimulated with vehicle or EGF (2 or 20 ng/ml) for 48 h. BrdU (1 μM) was added to the culture medium during the last 12 h (from 36 to 48 h after EGF treatment), 24 h (from 24 to 48 h after EGF treatment), 36 h (from 12 to 48 h after EGF

treatment) or 48 h (from 0 to 48 h after EGF treatment) of the exposure period. Thereafter, cells were fixed and processed for BrdU immunocytochemistry. The proportion of BrdU-labeled cells among all cells is shown. The data are means ± S.E.M. of six wells. *; significant difference from the 12-h group at each concentration of EGF ($p < 0.05$, One-way ANOVA followed by Dunnett's test). #; significant difference from the vehicle group for each BrdU exposure time ($p < 0.05$, One-way ANOVA followed by Dunnett's test).

Supplementary Fig. 3. The effect of PGD_2 on the cell death of NPCs. Dispersed NPCs from the primary neurospheres were seeded in LAB-Tek® chamber Slides pre-coated with poly-L-lysine followed by laminin, at a density of 4×10^5 cells/ml and cultured for 12 h in the absence of EGF. Subsequently, they were treated with or without various concentrations of PGD_2 (0.1–10 μM) in the presence of EGF (2 ng/ml) for 48 h. After cells were fixed with PFA, dead cells were visualized by TUNEL staining. Representative images (A) and the proportion of TUNEL (+)-cells (B) are shown. The data are means ± S.E.M. of three wells. *; significant difference from vehicle control ($p < 0.05$, One-way ANOVA followed by Dunnett's test). Scale bar = 200 μm.

Supplementary Fig. 4. The effects of PPARγ antagonists on the regulation of NPC proliferation by PGD_2. The details are the same as those in Supplementary Fig. 1 legend. After pretreatment with vehicle or the PPARγ antagonist GW9662 (0.1 μM) for 1 h, cells were stimulated with or without various concentrations of PGD_2 (0.1–10 μM) in the presence or absence of EGF (0, 2, 20 ng/ml) for 48 h. The data from the vehicle group was replotted from Supplementary Fig. 1. The data are means ± S.E.M. of three to four wells. *, ‡; significant difference from PGD_2-free (0 μM) in the vehicle or GW9662 group, respectively ($p < 0.05$, One-way ANOVA followed by Dunnett's test).

Supplementary Fig. 5. The effect of pretreatment with GSH-EE on the regulation of NPC proliferation by PGD_2. The details are the same as those in Supplementary Fig. 1 legend. The value of the control group was set to 100%. The data are means ± S.E.M. of three to four wells. #; significant difference from PGD_2-free (0 μM) in the vehicle group, †; significant difference from PGD_2-free (0 μM) in the GSH-EE group ($p < 0.05$, One-way ANOVA followed by Dunnett's test). *; significant difference between the vehicle and GSH-EE groups at each concentration of PGD_2 ($p < 0.05$, Student's *t*-test).

Supplementary Figure 1

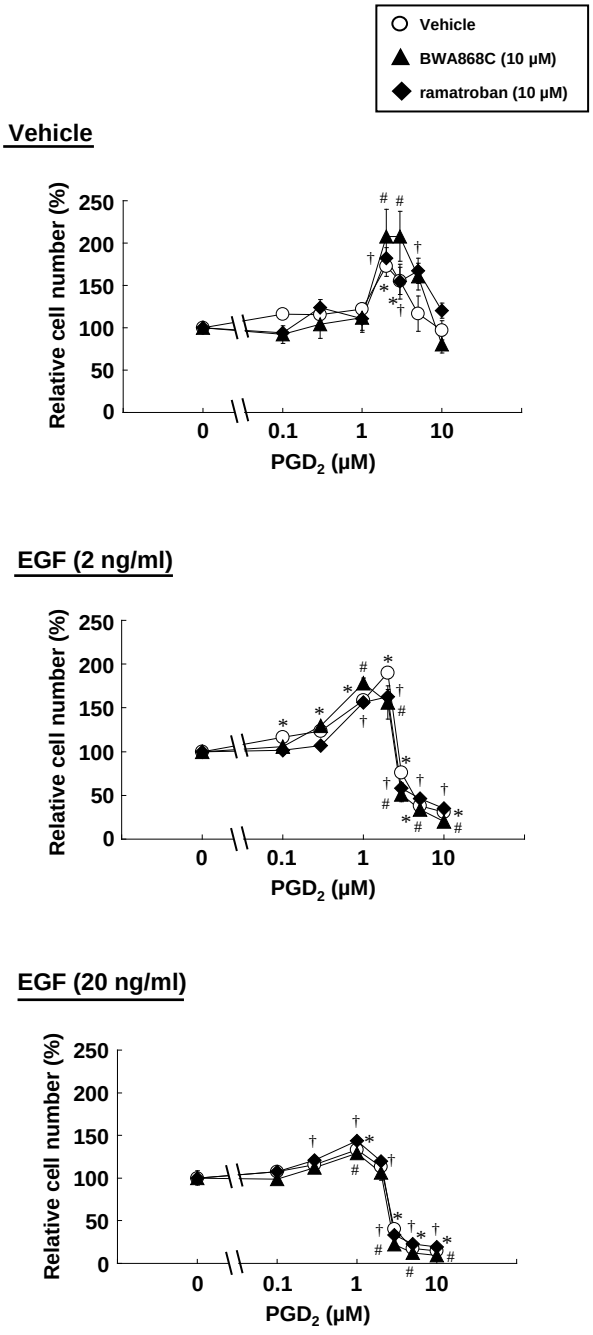

Supplementary Figure 2

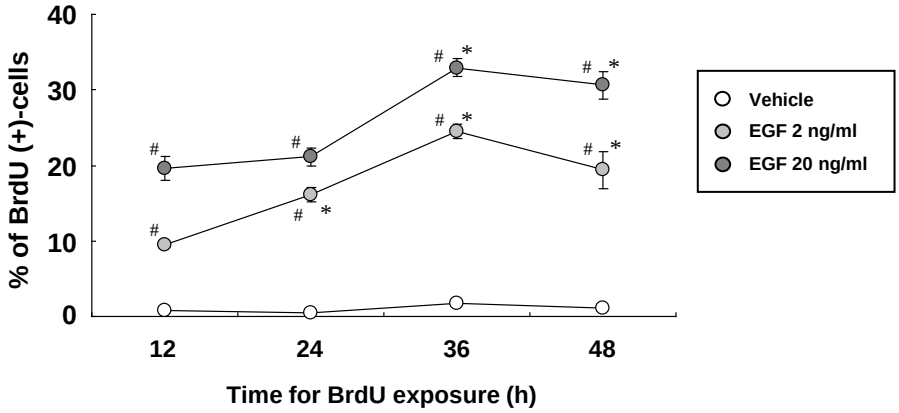

Supplementary Figure 3

(A) Representative images

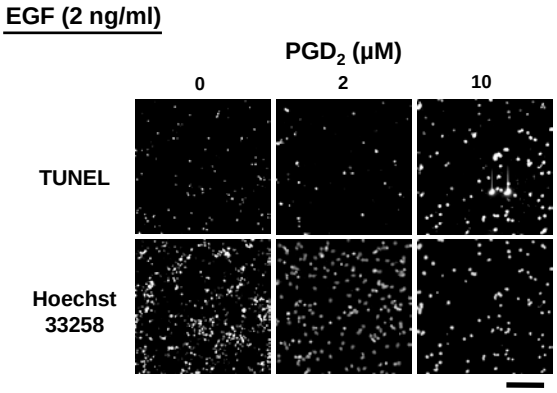

(B) Quantified data

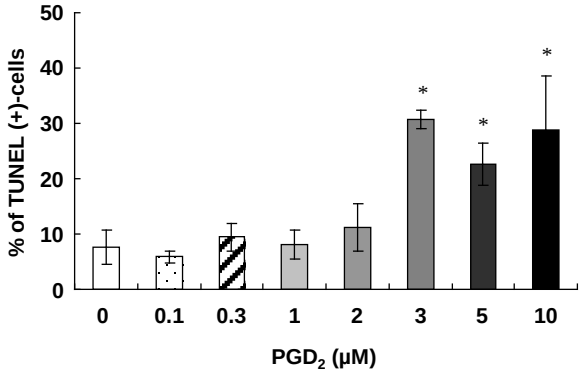

Supplementary Figure 4

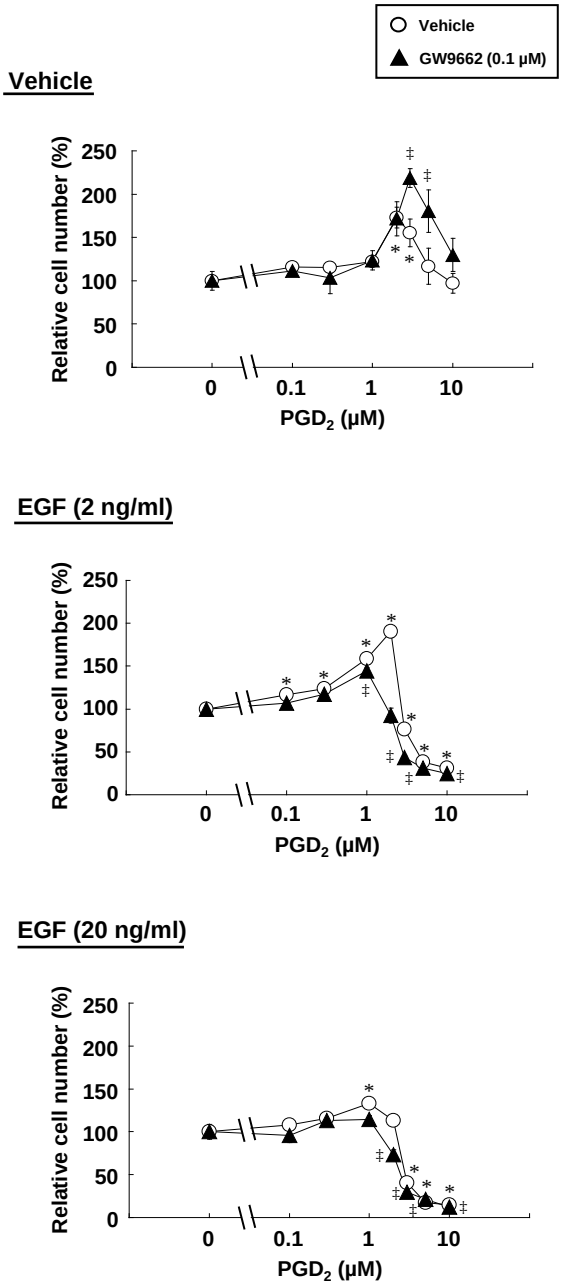

Supplementary Figure 5